

# n-type WO<sub>3</sub> semiconductor as a cathode electrochromic material for ECD devices

S. Hoseinzadeh<sup>1</sup> · R. Ghasemiasl<sup>1</sup> · A. Bahari<sup>2,3</sup> · A. H. Ramezani<sup>3</sup>

Received: 23 April 2017 / Accepted: 5 June 2017 / Published online: 24 June 2017  
© Springer Science+Business Media, LLC 2017

**Abstract** A new electrochromic (EC) arrangement is deposited on fluorine doped tin oxide (FTO) coated glass substrate by physical vapor deposition method. In this method, in the beginning, the WO<sub>3</sub> nanoparticles powder are deposited with average rate of 0.4 Å s<sup>-1</sup> in vacuum on FTO substrate for 80 min, then the Ag nanoparticles powder is deposited on prior layer for 1 min, again, the WO<sub>3</sub> electrochromic layer is deposited on prior layers for 5 min. In the end, the layer of Ag nanoparticles is deposited for 1 min with the rate of 0.1 Å s<sup>-1</sup>. The nanoparticles of WO<sub>3</sub> and Ag, as an n-type semiconductor acts as the cathode electrochromic material, while the nano-sized silver as a noble metal, plays the role of the electron trap centers to facilitate charge separation. That respectively have been used in fabricated electrochromic devices (ECDs), for this purpose, the temperatures of 100, 200 and 500 °C are selected and ECDs annealed for 2 min in vacuum. The thin film that annealed in 200 °C, exhibits good conductivity in cyclic voltammetry (CV) analysis and has a better EC performance. We obtain the maximum of current about 3.5 mA in oxidation state for this sample. Furthermore, the change of transmittance for this sample was upgraded to 40.30% at continuous switching steps. This arrangement (WO<sub>3</sub>/Ag/WO<sub>3</sub>/Ag) can be used in ECDs with its excellent properties.

## 1 Introduction

Over the last years, the global demand for energy has depended on fossil fuels, which can result in an energy crisis and contamination of the climate in the future. Therefore, the use of renewable energy sources obtained from sun, sea waves, wind, geothermal heat and other renewable sources have been growing for many different applications [1, 2]. However, perhaps the most economical solution is to use energy more efficiently. One efficient solution to make a feasible use of solar energy in buildings is to modify sunlight transmission through windows by solar-controlling coatings. Such solar-controlling coatings have chromogenic properties [3, 4]. The chromogenic materials used in solar-controlling coatings are electronic, optoelectronic, photochromic and thermochromic [1–5].

In brief, an electrochromic device (ECD) consists of several thin layers including transparent electrode, EC materials and electrolyte layer which are capable of changing the optical transmittance of ECD on switching the voltage [6–10]. The resulting optical transmittance changes revert to their original state when the polarity of the voltage is reversed by switching conversely. This phenomenon pertains to the injection and extraction of electrons and ions due to oxidation and reduction mechanism after applying different voltages ( $\leq 3$  V) [11–13].

As an inorganic material, tungsten oxide (WO<sub>3</sub>) is the most widely studied case in field of EC material, and has also had the greatest commercial uptake [14, 15]. Furthermore, WO<sub>3</sub>, as a nontoxic material, has fast response time, good intercalation properties (H<sup>+</sup>, Li<sup>+</sup>, Na<sup>+</sup> and K<sup>+</sup>), favorable coloration efficiency (CE) and desirable optical properties [16]. The reversible electrochromic effect in the case of WO<sub>3</sub> can be expressed as the following relation [17]:

✉ A. Bahari  
a.bahari@umz.ac.ir

<sup>1</sup> Department of Mechanical Engineering, West Tehran Branch, Islamic Azad University, Tehran, Iran

<sup>2</sup> Department of Physics, Faculty of Basic Sciences, University of Mazandaran, Babolsar, Iran

<sup>3</sup> Department of Physics, West Tehran Branch, Islamic Azad University, Tehran, Iran



Since the use of single metal oxide only limits the optimal performance of electrochromic phenomenon, the electrochromism of composite systems consist of noble metals and metal oxides can be used [18]. Such ECDs based on composite structures can be employed to modify electrochromic properties, compared to single metal oxides structures. In addition, researchers in EC field reported results such as the enhancement of CE as well as the durability for using composite structures [19, 20].

In the present work, we deposited the tungsten and silver powders as a famous EC metal oxide and a noble metal on FTO-coated glass to form a layer-by-layer structure using the physical vapor deposition (PVD) apparatus. The FTO–WO<sub>3</sub>–Ag–WO<sub>3</sub>–Ag thin films are prepared and the post-annealing processes are done in vacuum for 2 min at different temperatures including 100, 200 and 500 °C, to study the effects of temperature of post-annealing on electrochromic properties in this structure. The EC properties of the electrochromic thin films are investigated by cyclic voltammetry (CV), UV–vis spectra and current curves to illustrate reversible color changes and response time.

## 2 Experimental

### 2.1 Materials

Tungsten oxide (WO<sub>3</sub>) powder, Ag nanoparticles powder, lithium perchlorate, propylene carbonate (PC), hydrochloric acid, ethanol and acetone were purchased from Merck. The FTO-coated glass was purchased and cut into small pieces with the size of 2 × 0.9 cm<sup>2</sup>.

### 2.2 Instruments

Deposition of the thin films is done by PVD Apparatus (Meca 2000, France) that equipped with thickness gauge and operated in 10<sup>-6</sup>Torr. CV analyses are done by using the potentiostat at /galvanostatAutolab (Nova software model PGSTAT 302 N, Metrohm, Netherlands) coupled with a personal computer. The CV data are obtained in 0.5 M LiClO<sub>4</sub> in PC solution in which the FTO-coated glass slide is used as the working electrode, and a thin foil of platinum as well as Ag/AgCl (KCl saturated) are used as counters and reference electrodes, respectively. The morphology of the thin film was characterized by a field emission scanning electron microscopy (FESEM, model MIRA3 TESCAN, operated at 15 kV) and an atomic force microscopy (AFM, model: AP 0100, Park Scientific Instruments). Element identification results are obtained by energy disperse X-ray spectroscopy (EDX). The optical properties of the films are

investigated by UV–vis spectrophotometer (Shimadzu 210 spectrophotometer).

### 2.3 Preparation of electrochromic thin films

At first, the FTO-coated glasses are cleaned with common detergent and deionized water, HCl 0.1 M, ethanol, and finally acetone for 10 min in the ultrasonic bath in the room temperature. The partial of the FTO surface is masked to prevent of deposition in all of deposition process. Adequate amounts of WO<sub>3</sub> and Ag powder are laded into separated tungsten boats in PVD apparatus.

In the deposition process, the thickness and the rate of deposition are monitored by a digital thickness display monitor. Figure 1 shows the rates of deposition and applied current versus time. After 80 min, the thickness of the film increased to 200 nm. In the next process, Ag nanoparticles powder for 1 min, WO<sub>3</sub> nanoparticles powder for 5 min and Ag nanoparticles powder for 1 min are respectively deposited by PVD method. At the end of the deposition process, the multi-layer arrangement of electrochromic thin films (WO<sub>3</sub>/Ag/WO<sub>3</sub>/Ag) with the thickness of 200–2–10–2 Å are achieved. The post annealing processes are used to crevasse the Ag nanoparticles for 2 min in vacuum at 100, 200 and 500 °C.

## 3 Results and discussion

### 3.1 CV studies

Figure 2 shows the CV spectra of samples in 0.5 M LiClO<sub>4</sub>–PC solution in the potential region from –1.0 to +1.0 V (vs. Ag/AgCl) at a scan rate of 100 mV/s. It

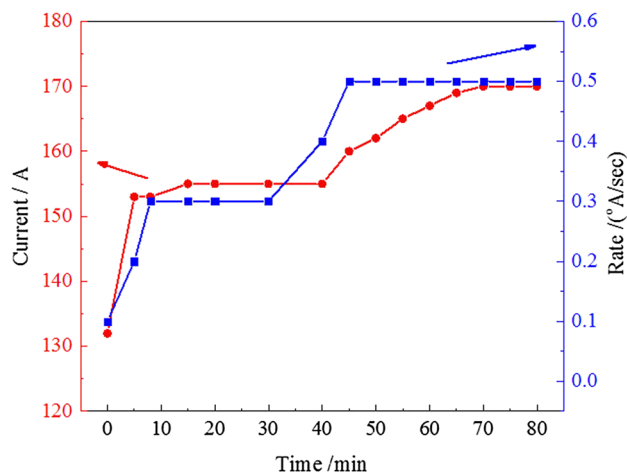


**Fig. 1** The curves of current and deposition rete versus time in deposition process

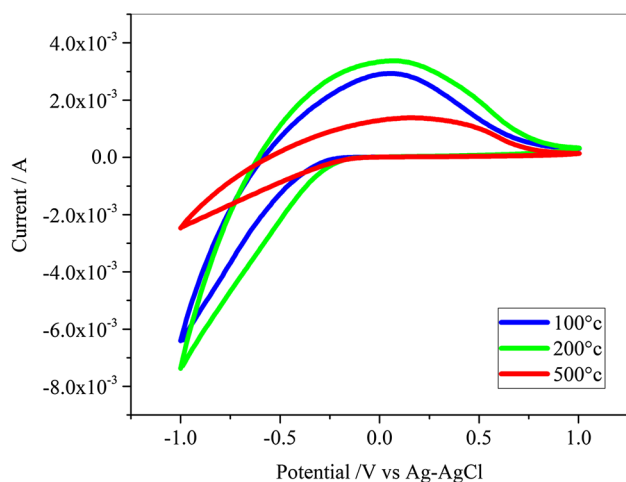


**Fig. 2** Cyclic voltammogram of electrochromic thin films in a 0.5 M solution of  $\text{LiClO}_4\text{-PC}$  at different post annealing temperatures

shows the effects of different post annealing temperatures on  $\text{FTO-WO}_3\text{-Ag-WO}_3\text{-Ag}$  electrochromic structures. All of samples exhibit one oxidation broad peak and one reduction broad peak due to the intercalation process of  $\text{Li}^+$  into, and the deintercalation of  $\text{Li}^+$  out from the nanocomposite thin films. As shown in Fig. 2, the oxidation broad peak shifted from +0.1 to +0.2 V when the temperature of post annealing increased from 100 to 500 °C. Furthermore, the sample with post annealing temperature of 200 °C has excellent conductivity at positive and negative potentials. On the other hand, the conductivity of sample with post annealing temperature of 500 °C strongly decreased.

#### 4 Morphology studies

The morphology of  $\text{WO}_3\text{-Ag-WO}_3\text{-Ag}$  thin film is characterized using FESEM and AFM. Figure 3 displays the FESEM and EDX images of sample. As can be seen, the sample consists of canaliculated surface with hills like shape (Fig. 3a). Among these canals, nanoparticles of silver can be seen with mean grain size of 24–45 nm (Fig. 3b). Furthermore, Fig. 3c shows the FESEM cross sectional picture of sample on FTO coated glass substrate. Figure 3d shows the EDX of sample that confirms the presence of fundamental elements for  $\text{FTO-WO}_3\text{-Ag-WO}_3\text{-Ag}$  sample. As it can be seen, the fundamental elements of tungsten oxide and silver with tin element (correlated to FTO layer) are present in EDX spectrum. In addition, the weight and atomic percentages of elements in structures of the samples are reported in Table 1. In order to study the topography of the sample surface, AFM analysis was done, and the result can be seen in Fig. 4. The morphology of the sample surface has an approximate roughness of 17 nm,

and Fig. 4 shows the hill-like structure that was previously seen in SEM pictures.

#### 4.1 EC properties

The optical transmittance of the prepared thin films at different post annealing temperatures changed at different applied DC voltage from  $-1.0$  to  $+1.0$  V. Fig. 5 shows and compares the visible optical transmittance spectrum of thin films at two applied DC voltages, the first in bleached state (blue curves) at  $+1.0$  V, and the second in colored state (red curves) at  $-1.0$  V. The maximum value of the optical transmittance of sample that annealed at 100 °C in bleached state is 76.93% at 632.8 nm while the minimum value of the optical transmittance in colored state is 46.95% in the same wavelength. The sample that were annealed at 200 °C shows a better result. The optical transmittance in bleached state is 81.15% at 632.8 nm, and the minimum value of the optical transmittance in colored state is 40.30% in the same wavelength. These results for the sample that were annealed at 500 °C are respectively 66.64 and 61.55%, that are briefly reported in Table 2. So, the differences of transmittance ( $\Delta T$  %) for  $\text{FTO-WO}_3\text{-Ag-WO}_3\text{-Ag}$  samples for post annealing temperatures at (100, 200 and 500) °C, respectively equal to 30.28, 41.07 and 5.12%. The coloration switching response is a very predominant parameter in EC materials. The switching time is computed as the time required for 90% change in the full transmittance modulation at 632.8 nm. Figure 6 shows the current transient response and the corresponding switching curves at 632.8 nm for  $\text{FTO-WO}_3\text{-Ag-WO}_3\text{-Ag}$  electrochromic thin films in 0.5 M  $\text{LiClO}_4\text{-PC}$  electrolyte. For all samples, the DC voltage steps were applied from  $-0.1$  to  $+1.0$  V, and subsequently, the response time for bleached and colored states are calculated as 13.8 and 10.1 s for sample at 100 °C, 15.6 and 9.5 s for sample at 200 °C and 14.2 and 29 s for sample at 500 °C. Figure 7 compares the current densities of electrochromic thin films at different sequential switching from  $+1.0$  to  $-1.0$  V and from  $-1.0$  to  $+1.0$  V. As it can be seen, the interchanged charge (area under the curve) in sample that post annealed at 200 °C is higher than other samples. In this case, current transient density through the electrochromic film at a consecutive switching in 30 s, started in about 4 ms for this nanocomposite, and it has a sharp drop to zero after the first few seconds. This result accompanied with the highest difference of transmittance ( $\Delta T$  %) for the sample that post annealed at 200 °C, introduce it as an optimal sample for this structure. In addition, we can compare the current densities of ( $\text{WO}_3$ ) and ( $\text{WO}_3\text{-Ag}$ ) thin films at different sequential switching from  $+1.0$  V to  $-1.0$  and from  $-1.0$  to  $+1.0$  V. In order to investigate the CE of samples; we use related equations as follow:

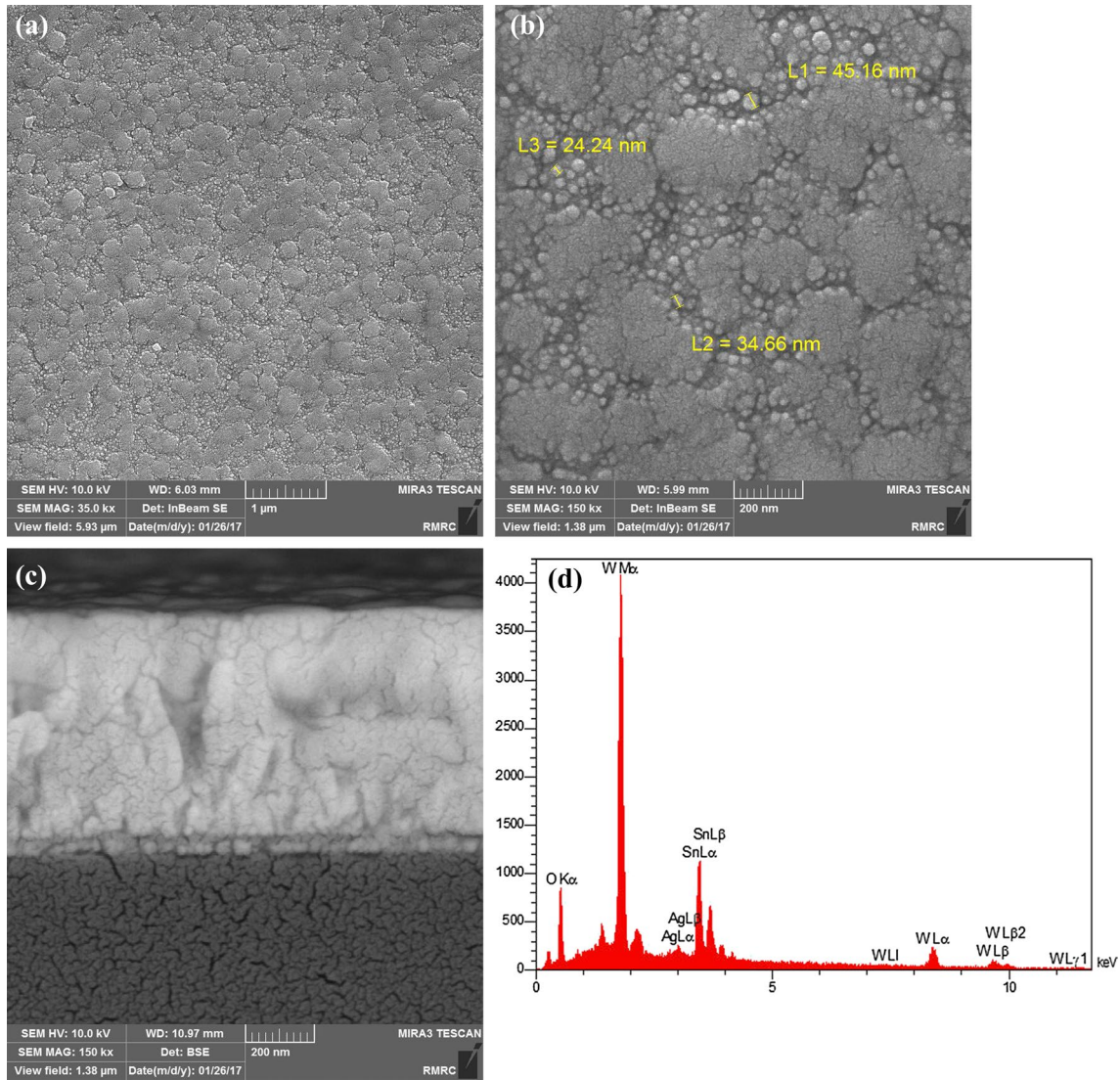


**Fig. 3** FESEM images of  $WO_3$ -Ag- $WO_3$ -Ag thin film (a and b) surface and c cross sectional, d EDX spectrum of sample

**Table 1** The detailed structures of the  $WO_3$ -Ag thin film

Sample	Element	W (%)	A (%)
$WO_3$ -Ag	O	19.30	69.84
	W	53.67	16.90
	Ag	1.60	0.86
	Sn	25.43	12.40

$$CE = \Delta OD / (Q/A) \tag{2}$$

$$\Delta OD(\lambda) = \log \frac{T_b}{T_c} \tag{3}$$

where  $T_c$  and  $T_b$  refer to the colored and bleached transmittances of the EC film [21, 22]. As shown in Fig. 8, the slope of the curves demonstrates the amount of CE [23]. The CE values of samples are calculated to be (61.2, 69.8 and 31.3)  $cm^2 C^{-1}$  for  $WO_3/Ag/WO_3/Ag$  thin films at 100, 200 and 500 °C (Fig. 9).

According to the experimental results of this section, it can be concluded that; at elevated temperatures such as 500 °C, two things happen: First, the tungsten oxide will be converted from amorphous state to a crystalline state and the electrochromic performance (current density and coloration efficiency) will be reduced in a crystalline state as compared to an amorphous state. Second, silver will be oxidized at high temperatures and this will reduce the performance (current density and coloration efficiency) of silver nanoparticles.



**Fig. 4** AFM image of WO<sub>3</sub>-Ag-WO<sub>3</sub>-Ag electrochromic thin film. Scan size is 0.5 × 0.5 μm

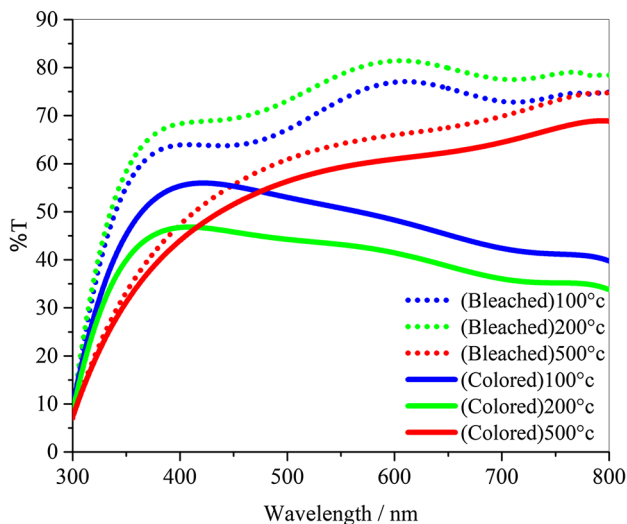
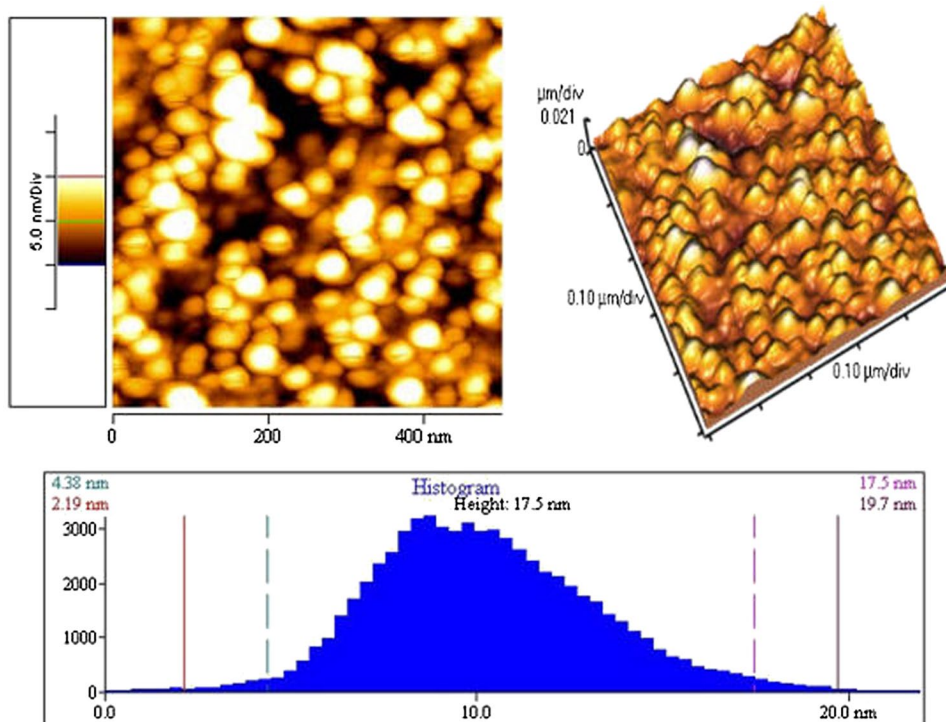


**Fig. 5** Visible transmittance spectra of WO<sub>3</sub>-Ag-WO<sub>3</sub>-Ag electrochromic thin films (at different post-annealing temperatures) under different potentials from -1.0 to +1.0 V

But at 200 °C, post heat treatment causes the silver particles be penetrate without of oxidation that formation of nanocomposite)silver tungsten oxide) will be improved the electrochromic performances (current density and coloration efficiency).

### 5 Conclusions

The thin film structures of WO<sub>3</sub>-Ag-WO<sub>3</sub>-Ag have been post-annealed at 100, 200 and 500 °C in vacuum for 2 min. The samples have been compared in EC properties. The results show that the obtained thin film at 200 °C has good conductivity and a better EC performance. Specially, the change of transmittance of this sample at 632.8 nm has increased to 40.30% at DC voltage steps -1.0 to +1.0 V in 0.5 M LiClO<sub>4</sub>-PC solution. Furthermore, the response time of this sample for bleached states has decreased to 9.5 s, and for colored states reached to 15.6 s at same DC voltage

**Table 2** Electrochromic properties of WO<sub>3</sub>-Ag-WO<sub>3</sub>-Ag thin films in 0.5 M solution LiClO<sub>4</sub>-PC at 632.8 nm for different post annealing temperatures

Sample (°C)	DC voltage steps (V)	T <sub>c</sub> (%)	T <sub>b</sub> (%)	ΔT (%)	τ <sub>c</sub> (s)	τ <sub>B</sub> (s)
100 °C	+1.0 ↔ -1.0	76.93	46.95	30.28	13.8	10.1
200 °C	+1.0 ↔ -1.0	81.15	40.30	41.07	15.6	9.5
500 °C	+1.0 ↔ -1.0	66.64	61.55	5.12	14.2	29

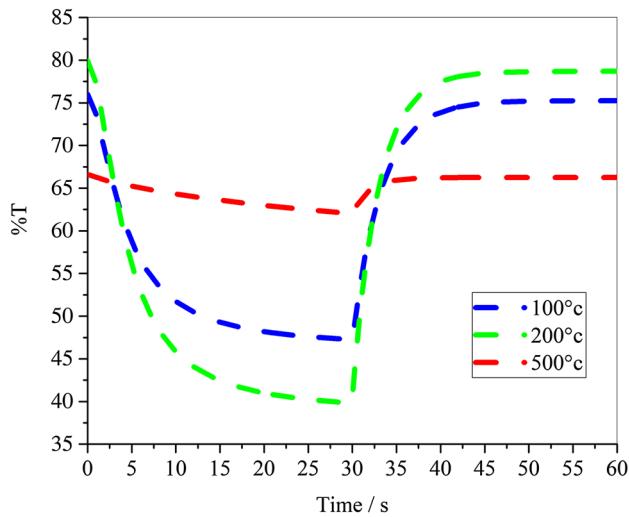


**Fig. 6** Electrochromic responses at 632.8 nm for  $\text{WO}_3\text{-Ag-WO}_3\text{-Ag}$  electrochromic thin films at different post annealing temperatures (-1.0 to +1.0 V) in 0.5 M  $\text{LiClO}_4\text{-PC}$  electrolyte

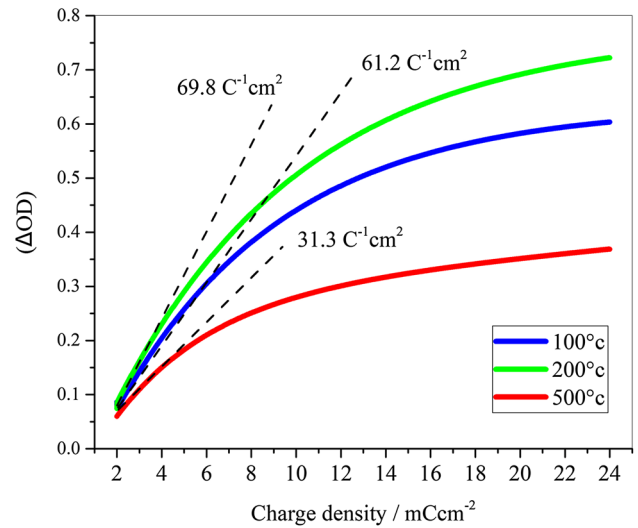


**Fig. 8** Variation of the in situ optical density (OD) versus charge density for  $\text{WO}_3\text{-Ag-WO}_3\text{-Ag}$  electrochromic thin films (at different post annealing temperatures)

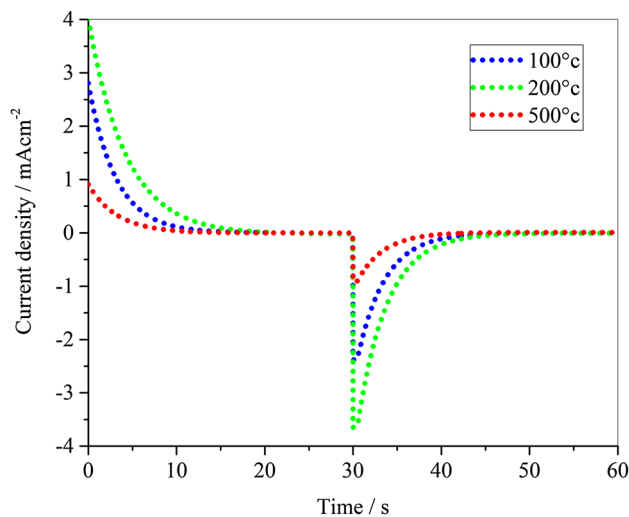


**Fig. 7** The current curves versus time for  $\text{WO}_3\text{-Ag-WO}_3\text{-Ag}$  electrochromic thin films at different post annealing temperatures (-1.0 to +1.0 V) in 0.5 M  $\text{LiClO}_4\text{-PC}$  electrolyte

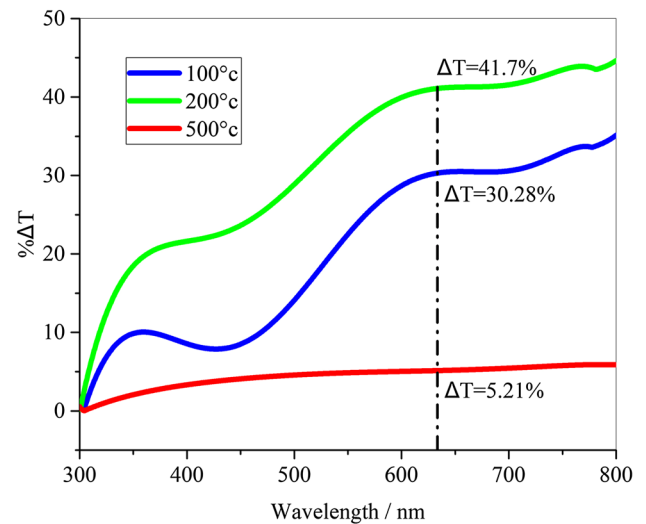


**Fig. 9** Optical transmittance differences of  $\text{WO}_3\text{-Ag-WO}_3\text{-Ag}$  electrochromic thin films versus wavelength (at different post annealing temperatures)

steps. CE of the sample that annealed at 200°C equals to  $69.8 \text{ cm}^2\text{C}^{-1}$ . This value of CE is suitable for industrial aspects.

**References**

1. R. Gholipur, ZKhorshidi, ABahari, Enhanced absorption performance of carbon nanostructure based metamaterials and tuning impedance matching behavior by an external AC electric field. *ACS Appl. Mater. Interfaces* **9**(14), 12528–12539 (2017)

2. M. Roeder, A.B. Beleke, U. Guntow, J. Buensow, A. Guerfi, U. Posset, H. Lorrmann, K. Zaghib, G. SEXTL,  $\text{Li}_4\text{Ti}_5\text{O}_{12}$  and  $\text{LiMn}_2\text{O}_4$  thin-film electrodes on transparent conducting oxides for all-solid-state and electrochromic applications. *J. Power Sources* **301**, 35–40 (2016)
3. H. Najafi-Ashtiani, A. Bahari, S. Ghasemi, A dual electrochromic film based on nanocomposite of copolymer and  $\text{WO}_3$  nanoparticles: enhanced electrochromic coloration efficiency and switching response. *J. Electroanal. Chem.* **774**, 14–21 (2016)
4. D. Dastan, S.L. Panahi, N.B. Chaure, Characterization of titania thin films grown by dip-coating technique. *J. Mater. Sci.* **27**(12), 12291–12296 (2016)

5. Y. Ren, Y. Gao, G. Zhao, Facile single-step fabrications of electrochromic  $\text{WO}_3$  micro-patterned films using the novel photosensitive sol–gel method. *Ceram. Int.* **41**(1), 403–408 (2015)
6. M. Nakhaei, A. Bahari, Synthesis and investigation of temperature effects on barium titanate ( $\text{BaTiO}_3$ ) nanostructural and electrical properties. *J. Mater. Sci.* **27**(6), 5899–5908 (2016)
7. D. Dastan, A. Banpurkar, Solution processable sol–gel derived titania gate dielectric for organic field effect transistors. *J. Mater. Sci.* **28**(4), 3851–3859 (2016)
8. M. Roodbari-Shahmiri, A. Bahari, H. Karimi-Maleh, R. Hoseinzadeh, N. Mirnia, Ethynylferrocene–NiO/MWCNT nanocomposite modified carbon paste electrode as a novel voltammetric sensor for simultaneous determination of glutathione and acetaminophen. *Sens. Actuators B* **177**, 70–77 (2013)
9. A. Bahari, R. Gholipur, Electrical and optical properties of  $\text{Zr}_x\text{La}_{1-x}\text{O}_y$  nanocrystallites as an advanced dielectric for the next FET devices. *J. Mater. Sci.* **24**(2), 674–686 (2013)
10. C.-G. Granqvist, G. A. Niklasson, A. Azens. Electrochromics: fundamentals and energy-related applications of oxide-based devices. *Appl. Phys. A* **89**(1), 29–35 (2007)
11. H. Li, Y. Lv, X. Zhang, X. Wang, X. Liu, High-performance ITO-free electrochromic films based on bi-functional stacked  $\text{WO}_3/\text{Ag}/\text{WO}_3$  structures. *Solar Energy Mater. Solar Cells* **136**, 86–91 (2015)
12. H. Najafi-Ashtiani, A. Bahari, S. Ghasemi, A dual electrochromic film based on nanocomposite of aniline and o-toluidine copolymer with tungsten oxide nanoparticles. *Org. Electron.* **37**, 213–221 (2016)
13. V.R. Buch, A.K. Chawla, S.K. Rawal. Review on electrochromic property for  $\text{WO}_3$  thin films using different deposition techniques. *Mater. Today* **3**(6), 1429–1437, (2016)
14. K. Sauvet, L. Sauques, A. Rougier, IR electrochromic  $\text{WO}_3$  thin films: from optimization to devices. *Solar Energy Mater. Solar Cells* **93**, 2045–2049 (2009)
15. S. Park, S. Kim, J. Choi, J. Song, M. Taya, S. Ahn, Low-cost fabrication of  $\text{WO}_3$  films using a room temperature and low-vacuum air-spray based deposition system for inorganic electrochromic device applications. *Thin Solid Films* **589**, 412–418 (2015)
16. C.-P. Cheng, Y. Kuo, C.-P. Chou, C.-H. Cheng, T.P. Teng, Performance improvement of electrochromic display devices employing micro-size precipitates of tungsten oxide. *Appl. Phys. A* **116**(4), 1553–1559 (2014)
17. M. Da Rocha, A. Rougier, Electrochromism of non-stoichiometric NiO thin film: as single layer and in full device. *Appl. Phys. A* **122**(4), 1–7 (2016)
18. K.W. Park, Electrochromic properties of Au– $\text{WO}_3$  nanocomposite thin-film electrode. *Electrochim. Acta* **50**, 4690–4693 (2005)
19. R.R. Kharade, S.S. Mali, S.P. Patil, K.R. Patil, M.G. Gang, P.S. Patil, J.H. Kim, P.N. Bhosale, Enhanced electrochromic coloration in Ag nanoparticle decorated  $\text{WO}_3$  thin films. *Electrochim. Acta* **102**, 358–368 (2013)
20. M.A. Gondal, M.A. Suliman, M.A. Dastageer, G.-K. Chuah, C. Basheer, Dan Yang, A. Suwaiyan, Visible light photocatalytic degradation of herbicide (Atrazine) using surface plasmon resonance induced in mesoporous Ag– $\text{WO}_3/\text{SBA-15}$  composite. *J. Mol. Catal. A* **425**, 208–216 (2016)
21. P.M. Kadam, N.L. Tarwal, P.S. Shinde, R.S. Patil, H.P. Deshmukh, P.S. Patil, From beads-to-wires-to-fibers of tungsten oxide: electrochromic response. *Appl. Phys. A* **97**(2), 323–330 (2009)
22. G.F. Cai, J.P. Tu, D. Zhou, J.H. Zhang, X.L. Wang, C.D. Gu. Dual electrochromic film based on  $\text{WO}_3/\text{polyaniline}$  core/shell nanowire array. *Solar Energy Mater. Solar Cells* **122**, 51–58 (2014)
23. S. Hoseinzadeh, R. Ghasemiasl, A. Bahari, A.H. Ramezani, The injection of Ag nanoparticles on surface of  $\text{WO}_3$  thin film: enhanced electrochromic coloration efficiency and switching response. *J. Mater. Sci.: Mater. Electron.* doi:[10.1007/s10854-017-7357-9](https://doi.org/10.1007/s10854-017-7357-9)